Ontogeny of collective behavior reveals a simple attraction rule

Robert C. Hinz[a,b] and Gonzalo G. de Polavieja[a,b,1]

[a]Champalimaud Research, Champalimaud Centre for the Unknown, 1400-038 Lisbon, Portugal; and [b]Cajal Institute, Consejo Superior de Investigaciones Cientificas, 28002 Madrid, Spain

Edited by Alan Hastings, University of California, Davis, CA, and approved January 13, 2017 (received for review October 12, 2016)

The striking patterns of collective animal behavior, including ant trails, bird flocks, and fish schools, can result from local interactions among animals without centralized control. Several of these rules of interaction have been proposed, but it has proven difficult to discriminate which ones are implemented in nature. As a method to better discriminate among interaction rules, we propose to follow the slow birth of a rule of interaction during animal development. Specifically, we followed the development of zebrafish, *Danio rerio*, and found that larvae turn toward each other from 7 days postfertilization and increase the intensity of interactions until 3 weeks. This developmental dataset allows testing the parameter-free predictions of a simple rule in which animals attract each other part of the time, with attraction defined as turning toward another animal chosen at random. This rule makes each individual likely move to a high density of conspecifics, and moving groups naturally emerge. Development of attraction strength corresponds to an increase in the time spent in attraction behavior. Adults were found to follow the same attraction rule, suggesting a potential significance for adults of other species.

collective behavior | interaction rule | zebrafish | development | shoaling

Collective animal behavior is studied with increasing detail in natural habitats (1–6) and laboratory conditions (7–14). Local interactions among animals can, in many cases, explain these patterns of collective behavior, and a variety of interaction rules have been proposed (7, 8, 11, 14–27).

One of the technical problems in discriminating among possible interaction rules is the difficulty of obtaining high-quality experimental data (25). We reasoned that the ontogeny of attraction behavior offers a unique opportunity to obtain a large high-quality dataset. This dataset should constrain the space of possible models to those that can explain interactions every day during development.

We turned to zebrafish, *Danio rerio*, a species in which larvae seem not to attract each other after hatching but that develop shoaling and schooling behavior during the first month of development (12, 14, 28–33). Our choice was based on our previous work in the adult suggesting a simplicity of the rules compared with other species (14).

In this work, we follow the formation of attraction behavior during the ontogeny of collective behavior in zebrafish. We used our newly developed tracking system of animals in groups, idTracker (34), in a total of 524 videos for the study of development and 25 videos for adults. We found that zebrafish are very weakly attracted to each other by 7 days postfertilization (dpf), and the attraction gets stronger each day during development. By 9 dpf, larvae are likely found close to each other, and, by 15 dpf, it is common to see animals moving in groups. Analysis and modeling of the developmental dataset point to attraction as turning toward a randomly chosen conspecific. Using this simple rule, animals are more likely to move toward high density of conspecifics without lumping, and group movement emerges. Development is found to correspond to an increasingly large amount of time spent in interaction behavior. We also found that the same rule can explain the behavior of freely moving adults, suggesting a potential significance for other species.

Results

We video-recorded isolated zebrafish and groups of two, four, or seven in an arena of 9 to 10 bodylengths (BL) of radius every day from 7 dpf, in which they start to swim, until 24 dpf (Fig. 1*A*; see Fig. S1*A* for setup). We used idTracker (34) to obtain the trajectory of each animal in a group using a method of image fingerprinting without the need for manual corrections (Fig. 1*B*). Correct identification of individuals is necessary for tests at the individual level but also to obtain the correct values of quantities derived from trajectory data like velocities or accelerations.

Ontogeny of Collective Behavior in Zebrafish. We first analyzed experiments that used pairs of zebrafish. A simple measure of whether two animals are interacting is given by their distance apart. We found that the most likely distance, or mode, is significantly lower than control randomized data from 9 dpf (Fig. 2*A*). The median distance is significant from 11 dpf (Fig. S1*B*), and the mean distance is significant from 12 dpf (Fig. S1*C*); this is because the distributions of distances are asymmetric, and the mode separates better data from control early in development (Fig. S1*D*).

We obtained similar results in the AB zebrafish strain, but significance in mode, median, and mean distance start from 11 dpf (Fig. S2). Also, the analysis can be given in terms of fish BL instead of age (Fig. S3).

Significance

Different interaction rules among animals can produce patterns of collective motion similar to those observed in bird flocks or fish schools. To help distinguish which rules are implemented in animal collectives, we studied the birth of the interaction rule in zebrafish during development from hatching to the juvenile stage. We used newly developed machine vision algorithms to track each animal in a group without mistakes. A weak attraction starts after hatching and gets stronger every day during development. Attraction consists in each larva moving toward one other larva chosen effectively at random and then switching to another one. This rule, simply by statistics, makes each individual move to regions of high density of individuals to produce collective motion.

Author contributions: G.G.d.P. designed research; R.C.H. and G.G.d.P. performed research; R.C.H. and G.G.d.P. analyzed data; G.G.d.P. wrote the paper; and R.C.H. wrote code and built the setup.

The authors declare no conflict of interest.

This article is a PNAS Direct Submission.

Freely available online through the PNAS open access option.

Data deposition: Data were deposited at www.idtracker.es/idsocial.

[1]To whom correspondence should be addressed. Email: gonzalo.polavieja@neuro.fchampalimaud.org.

This article contains supporting information online at www.pnas.org/lookup/suppl/doi:10.1073/pnas.1616926114/-/DCSupplemental.

ECOLOGY

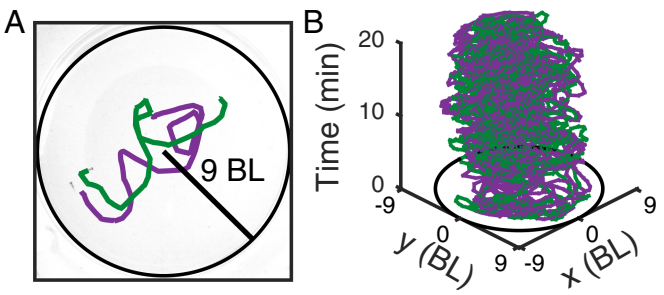

Fig. 1. Setup and tracking. (*A*) Setup of 9 to 10 BL radius. (*B*) Example of trajectory data for two zebrafish obtained from video using idTracker (34).

Interactions may depend not only on the distance between animals but also on the relative positions in space. Relative positions were studied using a coordinate system with origin on the focal animal and positive y axis pointing in the direction of its velocity vector (Fig. 2*B*, top left). We then computed the probability of finding the second animal in space (Fig. 2*B*; numbers indicate age). At 7 dpf to 11 dpf, animals spend significantly more time side by side than in front/back positions, and during 12 dpf to 24 dpf, they spend increasingly more time close to each other. Around the focal animal, there is also a region of low probability of finding the second animal (Fig. S1*E*). This region reduces size during development (Fig. S1*F*).

Distance and relative positions do not directly distinguish whether animals repel or attract each other. Attraction and repulsion can be studied more directly by measuring whether an individual accelerates toward or away from another individual (9, 10). As acceleration values change during development also for nonsocial interactions, we found it more useful to compute the probability of accelerating toward particular places. Specifically, we computed the probability (P_{turn}) that the focal turns to the side where the other fish is. This probability is significant from 7 dpf and increases during development (Fig. 3*A*). For the AB zebrafish strain, significance starts from 8 dpf (Fig. S2*D*).

More detail about attraction can be obtained studying the probability of turning to the right side depending on the location of the second animal (Fig. 3*B*). For 24 dpf, for example, the focal animal more often accelerates to the right (left) when the other animal is at its right (left) (Fig. 3*B*, day 24). This attraction structure starts to be significant at 6 dpf to 7 dpf and gets stronger during development (Fig. 3*B*).

Attraction can also be studied to the front or back position (Fig. S4), giving that, at 10 dpf to 24 dpf, animals accelerate to another animal in front and brake when behind, and, at 6 dpf to 9 dpf, there is some repulsion from an animal behind (Fig. S4*B*).

Using Development to Extract the Rule of Attraction. We used experiments with four fish to find whether there is an attraction rule that can explain the data. We found best correspondence by a model in which each animal interacts a proportion of the time by moving toward a randomly chosen individual (Fig. 4*A*). According to this model, when a focal has N_1 animals to one side and N_2 animals to the other, the probability of choosing the side with N_1 animals would be given by

$$P(N_1|N_1:N_2) = p_s\frac{N_1}{N_1+N_2} + (1-p_s)\frac{1}{2}, \qquad [1]$$

and $P(N_2|N_1:N_2) = 1-P(N_1|N_1:N_2)$ for the other side. This probability has two contributions. The first contribution comes from the proportion of time p_s spent in interactions in which the focal chooses one animal at random and thus the side with N_1 animals with probability $N_1/(N_2+N_2)$. The second contribution comes from the remaining proportion of time, $1-p_s$, in which the focal does not interact with other animals, giving, in our experiments, in which no consistent left–right asymmetry exists, a probability $1/2$ for each side.

The model in Eq. **1** has one parameter, the time spent in interactions, p_s, but also makes predictions independent of this parameter. For experiments using four animals, a focal fish can be found with zero and three fish to its sides (configuration 0:3) or one and two fish (configuration 1:2). The model predicts a relationship between the probabilities for these two configurations that is independent of the parameter as

$$P(1|1:2) = \frac{1}{3} + \frac{1}{3}P(0|0:3), \qquad [2]$$

plotted as a solid red line in Fig. 4*B*. Another relationship is the one between the probability of turning to the side of no animals for these experiments with four animals and those experiments with only two animals as

$$P(0|0:3) = P(0|0:1), \qquad [3]$$

plotted as a solid blue line in Fig. 4*C*. The general parameter-free relationship between two probabilities can be found in *Methods*.

We checked that these theoretical predictions in Eqs. **2** and **3** are also seen in agent-based simulations in which each agent

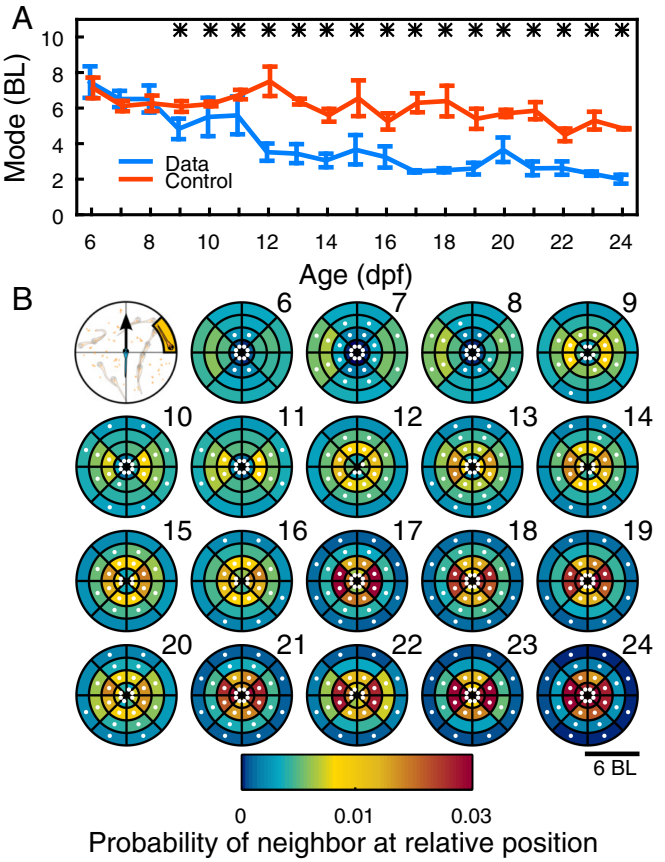

Fig. 2. Development of distance and relative position between two fish. (*A*) Most likely distance between pairs of fish at ages 6 dpf to 24 dpf (blue), N = 4 to 12 pairs per day, and same for control randomized data (orange). Data are mean SEM. Stars indicate $P < 0.05$. (*B*) Focal animal is at the center of the coordinate system, with velocity vector pointing in the direction of y axis (top left). Other images show probability of finding second animal in space for ages 6 dpf to 24 dpf. Data are mean for each age, with age indicated by numbers 6 to 24. Dots indicate regions with $P < 0.005$.

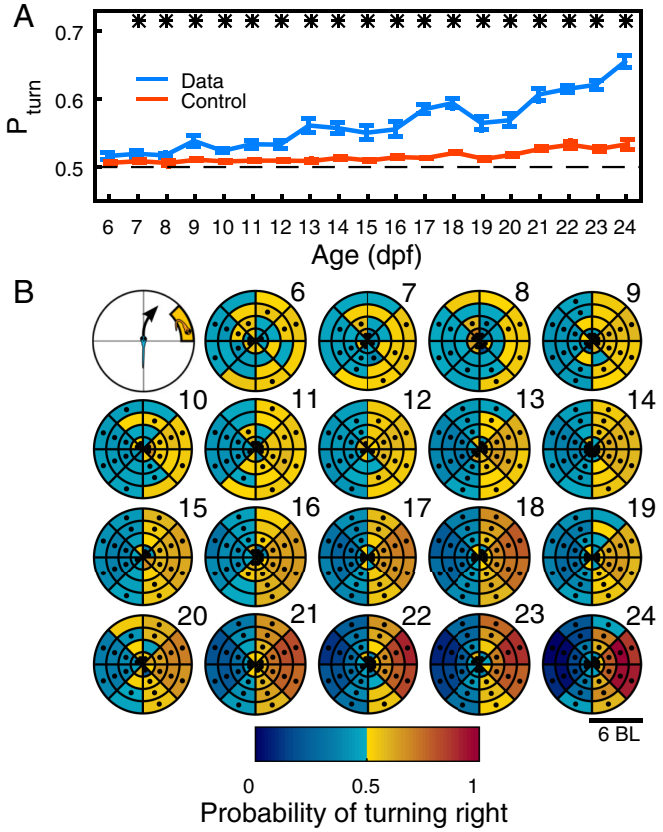

Fig. 3. Development of attraction. (*A*) Probability of accelerating toward the side in which the other animal in the pair is located (blue), and control randomized data (orange) from 6 dpf to 24 dpf. Data are mean, and error bars are SEM. Stars indicate days with $P < 0.05$. (*B*) Probability of focal animal turning right when second animal is in different positions in space. Focal animal is at the center of the coordinate system, with velocity vector pointing in the direction of *y* axis. Data are mean for each age, with age indicated by numbers 6 to 24. Dots indicate regions with $P < 0.005$.

turns with probability p_s to the side of another agent chosen at random and, with probability $1 - p_s$, turns left or right randomly (Fig. S5*B*, dots for different values of p_s; see *Methods* for details of simulations).

For the analysis of the experimental data, we realized that the probability of turning to one side is random when another animal is very close, increases with the distance to another animal, and, at >2.5 BL, is independent of distance (Fig. S6*A*). As for this first analysis we are not considering space dependencies of attraction, we used only data when animals are at >2.5 BL from the focal. We found that these experimental data correspond well with the theoretical predictions in Eq. **2** (Fig. 4*B*) and Eq. **3** (Fig. 4*C*), with different days marked with corresponding numbers.

Another prediction of the interaction rule in Eq. **1** is that the probability of turning to the side with N_1 animals grows linearly with N_1 as $N_1/(N_1 + N_2)$. Groups of four animals only have two possible configurations, $(0 : 3)$ and $(1 : 2)$, so, for a proper test of this linearity, we used the four configurations arising in groups of seven fish (Fig. 4*D*).

We also checked that animals do not favor turning toward the side with the closer, intermediate, or farthest neighbor. The probability that the side chosen is the one with the closest animal is found to be very similar to the probability that it is the side with the animal at intermediate distance or the side with the farthest animal during all development (Fig. 4*E*). Our agent-based simulations with agents turning to another randomly chosen agent also give this result (Fig. S5*B*, column 4).

We simulated alternative agent-based models with one of eight other interaction rules, including turning to the side with more animals (Fig. S5*C*), to the side of the center of mass of the rest of the group (Fig. S5*D*), to the closest animal (Fig. S5*E*), to the center of mass of the two closest neighbors (Fig. S5*F*), to the second neighbor (Fig. S5*G*), and to the third neighbor (Fig. S5*H*), and using the nonlinear decision rules from ref. 14 (Fig. S5*J*) and ref. 21 (Fig. S5*I*). We found worse correspondence with experimental data using any of these eight rules in Fig. S5*C*–*J* than the theoretical predictions from Eq. **1** (Fig. S5*A*) or its implementation with agents turning toward one animal chosen at random (Fig. S5*B*).

N_1 Using the Attraction Rule for a Quantitative Description of Development. Once we tested the parameter-free predictions of the model, we used its "attraction" parameter p_s in Eq. **1** to give a compact description of changes during development. For each day t_i, we computed three values for $p_s(t_i)$ by fitting Eq. **1** to the experimental probabilities $P(2|2:1)$, $P(0|0:3)$, and $P(0|0:1)$ of that day and computed its mean value (Fig. 4*F*, dots). The value of the attraction parameter increases rapidly during development and could be fitted for the period 6 dpf to 24 dpf with the exponential $\exp((x - 28.6)/6)$ (Fig. 4*F*, line).

Inserting $p_s = \exp((x - 28.6)/6)$ into Eq. **1**, one obtains that the change during development of the different probabilities obtained in groups of two and four fish is expected to be of the form

$$P(2|1:2)(t) = \frac{1}{2}\exp((x - 28.6)/6) + \frac{1}{2} \qquad [4]$$

$$P(3|0:3)(t) = P(1|0:1) = \frac{1}{6}\exp((x - 28.6)/6) + \frac{1}{2}. \qquad [5]$$

These expressions correspond well with the experimental development of the probabilities $P(1|0:1)$, $P(3|0:3)$, and $P(2|1:2)$ (Fig. 4*G*).

We also performed experiments on adult zebrafish of 150 dpf to assess how developed interactions are by 24 dpf. For example, the attraction parameter p_s increases exponentially from a value of 0.01 at 6 dpf to a value of 0.47 at 24 dpf, but only has a very small increase to a value of 0.54 in the adult stage of 150 dpf (Fig. S7*A*). The other parameters measuring interaction also have values at 24 dpf close to those at 150 dpf (Fig. S7).

Agent-Based Modeling. We used the agent-based model to test further the ability of the attraction rule in Eq. **1** to explain experiments. Agents turn in the direction of a randomly chosen neighbor with probability p_s (taking values from Fig. 4*F*), whereas, with probability $1 - p_s$, they choose randomly to turn left or right. As the model was designed to describe the turning dynamics, we expected that turning properties would correspond well to experiments (Fig. S8*A* and *B*).

We also expected that agents would come together, and more so the higher the value of p_s. It is less obvious that the model can give a quantitative description of aggregation properties, as these could depend on other factors apart from the turning properties. However, the match between simulations and experiments was found to be quantitative for the most likely distance between two fish (Fig. 5*A*), their mean distance (Fig. S8*C*), the distributions of distances (Fig. S8*D*), and the relative positions (Fig. S8*E*).

We also tested for the formation of groups of different sizes, defined by how many animals are together at a distance, say, of less than 6 BL. Simulations predicted, for example, that it is only from 18 dpf that the most common group configuration in experiments with four animals should be groups of 4 (Fig. 5*B*, *Top*), and this is also seen in experiments (Fig. 5*B*, *Bottom*).

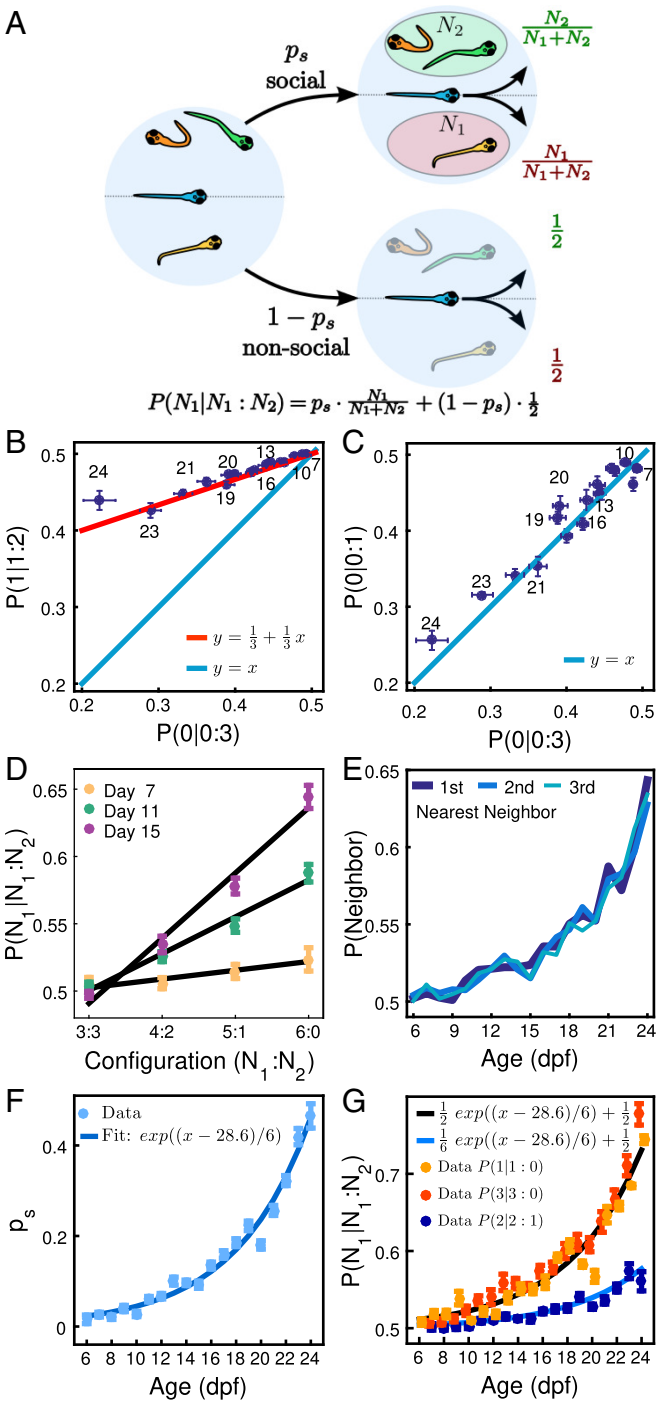

Fig. 4. Attraction rule from developmental data. (*A*) Diagram of model in which individuals spend a proportion of time p_s in interactions consisting in turning toward one animal chosen at random and time $1-p_s$ not interacting. Probability of moving to the side with N_1 animals is then Eq. **1**. (*B*) Relationship between the probability of turning to the side of 1 animal in a configuration (1:2), $P(1|1:2)$, and the probability of turning to the side of no animals in a configuration (0:3), $P(0|0:3)$. Blue dots indicate experimental data, with numbers indicating age in dpf. Red line indicates theoretical line in Eq. **2**. (*C*) Relationship between turning to the side of no animals in experiments with two and four fish, $P(0|0:1)$ vs. $P(0|0:3)$. Blue dots indicate experimental data, with numbers indicating age in dpf. Blue line indicates theoretical line in Eq. **3**. (*D*) Probability of turning to side with three, four, five, and six animals in a group of seven animals for days 7, 11, and 15. (*E*) Probability that the side chosen by an animal corresponds to the closest, intermediate, or farthest neighbor. (*F*) Parameter p_s as extracted fromthe data (dots) and fit to an exponential (line). (*G*) Probabilities $P(1|1:0)$, $P(3|3:0)$, and $P(2|2:1)$ during development. Lines are Eqs. **4** and **5**.

Finally, we used simulations to test interaction models more complex than Eq. **1**. We had seen in the data that attraction depends on distance to another fish for a distance less than 2.5 BL (Fig. S6*A*), but we ignored it in our analysis using Eq. **1**. A second feature seen in experiments is some repulsion from behind the focal animal (Fig. S4*B*), and, again, this was ignored in our analysis using Eq. **1**. Simulations including these two additional features gave results very similar to those of the simpler version (Fig. S9).

Discussion

Attraction among zebrafish was found to start at 7 dpf; by 9 dpf, they are likely found close to each other, and, by 2 weeks, they swim in groups.

We used this dataset of development of interactions to test the parameter-free predictions of a model according to which animals spend part of the time in interactions with conspecifics by turning toward an animal chosen at random. The interaction rule makes each animal likely initiate motion toward a high density of animals.

We also found that our proposed rule corresponds well to adult behavior in our freely moving experiments (Fig. S7), even better than a rule we had previously obtained specifically for adult zebrafish (Fig. S5*J*). We thus suggest that our rule may be relevant in other species.

An important element of our rule in Eq. **1** is that each animal is not interacting at all times. The only parameter of our rule is p_s, which measures the probability of interaction. At 6–7 dpf, the p_s value is very close to zero (Fig. 4*F*), and this translates into animals spending most of their time doing something different than interacting with other animals. The value of p_s increases exponentially until 24 dpf to a value of 0.47, similar to the adult value of 0.54. These values of p_s correspond to animals interacting with a probability close to 0.5, avoiding lumping without the need for a strong repulsion. In fact, most changes during development can be explained simply by an increase in the amount of time spent in interactions (Fig. 4*F*). Adding two extra features seen in the experiments, a reduced attraction at <2.5 BL and a weak repulsion from behind at early stages, gives results very similar to those of the simpler rule alone.

Our rule bears some resemblance to rules from the selfish herd hypothesis (15) used to explain tight group formations in the presence of a predator at an unknown location (35–40). Hamilton considered moving to the center of mass of the two closest neighbors as the ideal rule and moving to the closest neighbor as a simpler rule. These two rules make animals lump together, but adding to them a probability to interact lower than 1, as we did for Eq. **1**, avoids lumping and brings the modified rule closer to our data. We have tested these two rules and six other variants, and found a worse correspondence than with our proposed rule (Fig. S5). Nevertheless, the ideal rule of Hamilton corresponded well with our data for the relationship between turning probabilities (Fig. S5*F*, columns 1 and 2). The turning probabilities themselves are, however, more nonlinear than the experimental ones (Fig. S5*F*, column 3). This rule also favors the two closest neighbors more than seen in the experiments (Fig. S5*F*, column 4).

Our results suggest that collective behavior may be driven by an attention-like mechanism by which each individual in a group selects one out the many images of conspecifics. As we found attraction early in development, one could take advantage of the high transparency of zebrafish larvae to perform image processing of social information in neuronal circuits (41–43). A natural extension of attention mechanisms to more complex rules of interaction in other contexts or species is to consider biases in

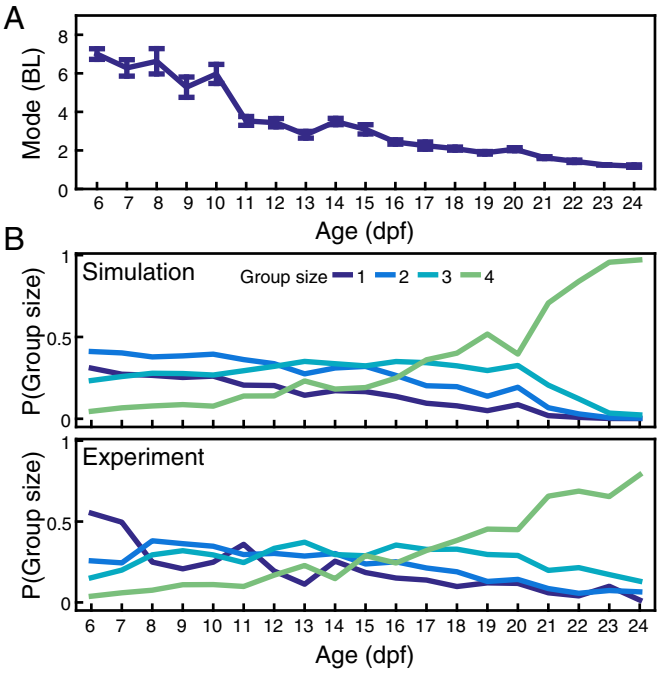

Fig. 5. Aggregation from agent-based simulations. (*A*) Most likely distance or mode between pairs of agents at ages 6 dpf to 24 dpf (blue), $N = 8$ pairs per day. Data are mean, and error bars are SEM. (*B*) For 4 individuals, probability of finding groups of one, two, three, or four individuals at less than 6 BL, for simulations and experiments. See *Methods* for details of simulations.

attention by a variety of properties of the other animals, including their distance, speed, direction of movement, or body posture.

Methods

Trajectories of individuals in groups for the 549 videos and analysis routines named as idSocial package can be obtained from www.idtracker.es/idsocial.

Housing and Maintenance. We used wild-type zebrafish from ZF Biolabs and the AB strain. Animals were kept in Petri dishes of 15 cm diameter inside an incubator with a 14/10 light–dark cycle until 5 dpf at 27.5 °C. Larvae were given powder food (sera micron) three times a day once they had started foraging. Excess food and debris were removed twice a day, and one third of the water was replaced with fresh system water. At 5 dpf, zebrafish larvae were transferred to the experimental setup (Fig. S1*A*) consisting of an external tank of dimensions 95 × 135 × 30 cm containing 180 L of system water at 27.5 °C, filtered and heated by an external filter system (Fluval 406, Teco TR 5). This external tank contained two 12 × 12 × 30 cm holding tanks, submerged up to 2/3 of their height in the water of the external tank to keep temperature constant. A weak flow of fresh water was delivered from the external tank. Each holding tank had approximately 100 larvae. During the experiments, only larvae from the same holding tank were grouped together. Water temperature and light–dark cycle were kept the same as in the incubator. The feeding protocol stayed the same as in the incubator until 12 dpf, when, for the midday feeding, the powder food was replaced by live artemia. Adults were transferred to the experimental setup 48 h before starting the experiments. They were kept in two 25 × 10 × 15 cm holding tanks, each holding 25 fish. They were fed dry food three times a day. All other conditions were the same as for larvae.

Recording Conditions. Videos were recorded with a Basler 622f camera and a Zeiss 16-mm objective. We used a watch glass as experimental arena, as animals spend less time in its borders compared with a Petri dish. It was placed at the center of a transparent Plexiglas board, which was submerged enough to cover the watch glass from below to keep the temperature constant and to reduce reflections at the air–glass boundary. Before each new trial, the watch glass was taken out of the setup and cleaned. It was then filled with a small volume of system water, and animals were transferred to it from holding tanks. BL of all larvae in the arena was determined using a custom-made script (www.idtracker.es/idsocial) to manually select snout and tail of each animal. Another custom script used the mean BL to plot a circle of radius 9 to 10 BL on the live camera image to mark the desired borders of the arena, and system water was added to this target. The height of the camera was then adjusted until the arena covered the whole image, resulting in a BL of ∼50 pixels for each animal. The homogeneity of the illumination was checked using a custom-made script (www.idtracker.es/idsocial), which simulated the background/foreground segmentation of idTracker (34) to guarantee tracking quality. We then recorded a 20-min video for each trial. For adults, we used a custom-made acrylic arena in the shape of a watch glass with diameter 75 cm and maximum depth of 6.5 cm. Experimental protocol was as for larvae.

Computation of Trajectories. The output of idTracker (14) is the center of mass of each animal for each frame. *SI Text* and Fig. S10 give the procedure for trajectory smoothing by a moving average. The velocity vector of an individual in frame t is then calculated from its smoothed trajectory as the difference between its x–y coordinate in frame t and frame $t-1$, $\vec{v}(t) \propto [x(t+1), y(t+1)] - [x(t), y(t)]$, and acceleration is calculated as $\vec{a}(t) \propto \vec{v}(t+1) - \vec{v}(t)$. Using distance, relative distance, and these velocity and acceleration vectors, the toolbox idSocial (downloadable from www.idtracker.es/idsocial) gives a variety of methods to study interactions, including those used in this paper (Fig. S11).

Control Randomized Data. Control data are obtained by randomization of the original data. For any video of two animals with N frames, we paired the position of fish 1 in each frame t_i, $x_1(t_i)$, with the position of fish 2 in a random frame $t_{\text{rand},\,i}$ separated from t_i by at least 16, 000 frames to avoid any correlations, $x_2(t_{\text{rand},\,i})$. From the video with N frames, we then get the N pairs $[x_1(t_i), x_2(t_{rand,\,i})]$. Repeating this 20 times with different random numbers and also for fish 2 instead of fish 1, we get 40 versions of the N pairs $[x_1(t_i), x_2(t_{rand,\,i})]$, equivalent to having 40 control randomized videos per experimental video.

For control randomized data in the study of acceleration of the focal, $a_1(t_i)$, depending on position of the second fish, we used analogous procedure to obtain the pairs $[a_1(t_i), x_2(t_{rand,\,i})]$.

Significance Tests. Significance is then obtained as the probability that the control randomized data give the experimental result. Using the procedure to build control randomized data, if, for a given age, we have M videos, we then obtain $40 \times M$ control videos. We illustrate in the following how to use these control videos for a significance analysis of the mean distance between two fish at a given age. For each of the M experimental videos of fish pairs taken at that age (say $M = 10$), we obtain a mean distance, giving 10 values of mean distance, whose mean is d_{exp}. From the 400 control videos, we extract 400 mean distance values. We then draw 10 random values from these 400 and compute their mean, d. This is repeated 10, 000 times, giving 10, 000 values of d and we compute the P value as the proportion of these 10, 000 with values equal to or smaller than the experimental value, $P(d \leq d_{eq})$.

For probability maps, we run an analogous procedure, but using 1, 000 repetitions for each bin of the map.

Parameter-Free Relationship Between Pairs of Configurations. Eq. **1** implies a parameter-free relationship between any pair of asymmetric configurations ($N_1 : N_2$ with $N_1 \neq N_2$ and $\bar{N}_1 : \bar{N}_1$ with $\bar{N}_1 \neq \bar{N}_2$) as

$$P(N_1|N_1 : N_2) = \frac{1}{2} + \frac{(N_1 - N_2)(\bar{N}_1 + \bar{N}_2)}{(N_1 + N_2)(\bar{N}_1 - \bar{N}_2)} \left(P(\bar{N}_1|\bar{N}_1 : \bar{N}_2) - \frac{1}{2} \right). \quad [6]$$

Eqs. **2** and **3** are two particular cases of this expression.

Calculation of the Mode. We used kernel density estimation with an Epanechnikov kernel and a bandwidth of two BL to obtain smooth continuous distributions from which the value with maximum probability was calculated.

Agent-Based Model. The movement of N agents is simulated by fixing a set of rules for the interaction among them and with the borders of the arena. Agents move at constant speed and turn a fixed angle in the direction of a randomly chosen neighbor with probability p_s, whereas, with probability $1 - p_s$, they choose randomly to turn left or right. The correspondence between the value p_s and day of development is as in the data from Fig. 4*F*. Fig. S5 uses alternative interaction rules. For the nonsocial part of the model, we used as constant speed the mean experimental speed (Fig. S6*B*), the turning at a relevant experimental value (Fig. S6*C*), and interactions with the borders of arena mimicking experimental ones (*SI Text*).

ACKNOWLEDGMENTS. We thank Mattia Bergomi, Iain Couzin, Andres Laan, Alfonso Perez-Escudero, and Michael Orger for discussions; Isidro Dompablo (CSIC) and Ana Catarina Certal (Fundação Champalimaud) for animal care; and Paulo Carriço (Fundação Champalimaud) for technical assistance with setups. This work was supported by Spanish Plan Nacional Ministerio de Economia y Competitividad Grants BFU2012-33448 and BFU2013-49512-EXP (to G.G.d.P.), Fundação para a Ciência e Tecnologia PTDC/NEU-SCC/0948/2014 (to G.G.d.P.), and Fundação Champalimaud (to G.G.d.P.). The funders had no role in study design, data collection and analysis, decision to publish, or preparation of the manuscript.

1. Krause J, et al. (2000) Fish shoal composition: Mechanisms and constraints. *Proc R Soc London Ser B* 267(1456):2011–2017.
2. Croft DP, et al. (2003) Mechanisms underlying shoal composition in the Trinidadian guppy, *Poecilia reticulata*. *Oikos* 100(3):429–438.
3. Ballerini M, et al. (2008) Interaction ruling animal collective behavior depends on topological rather than metric distance: Evidence from a field study. *Proc Natl Acad Sci USA* 105(4):1232–1237.
4. Nagy M, Akos Z, Biro D, Vicsek T (2010) Hierarchical group dynamics in pigeon flocks. *Nature* 464(7290):890–893.
5. Attanasi A, et al. (2014) Collective behaviour without collective order in wild swarms of midges. *PLoS Comput Biol* 10(7):e1003697.
6. Strandburg-Peshkin A, Farine DR, Couzin ID, Crofoot MC (2015) Shared decision-making drives collective movement in wild baboons. *Science* 348(6241):1358–1361.
7. Ward AJW, Sumpter DJT, Couzin ID, Hart PJB, Krause J (2008) Quorum decision-making facilitates information transfer in fish shoals. *Proc Natl Acad Sci USA* 105(19):6948–6953.
8. Sumpter DJT (2010) *Collective Animal Behavior* (Princeton Univ Press, Princeton).
9. Katz Y, Tunstrøm K, Ioannou CC, Huepe C, Couzin ID (2011) Inferring the structure and dynamics of interactions in schooling fish. *Proc Natl Acad Sci USA* 108(46):18720–18725.
10. Herbert-Read JE, et al. (2011) Inferring the rules of interaction of shoaling fish. *Proc Natl Acad Sci USA* 108(46):18726–18731.
11. Perna A, et al. (2012) Individual rules for trail pattern formation in Argentine ants (*Linepithema humile*). *PLoS Comput Biol* 8(7):e1002592.
12. Miller N, Gerlai R (2007) Quantification of shoaling behaviour in zebrafish (*Danio rerio*). *Behav Brain Res* 184(2):157–166.
13. Romenskyy M, Herbert-Read JE, Ward AJW, Sumpter DJT (2015) The statistical mechanics of schooling fish captures their interactions. arXiv:1508.07708.
14. Arganda S, Pérez-Escudero A, de Polavieja GG (2012) A common rule for decision making in animal collectives across species. *Proc Natl Acad Sci USA* 109(50):20508–20513.
15. Hamilton W (1971) Geometry for the selfish herd. *J Theor Biol* 31(2):295–311.
16. Vicsek T, Czirok A, Ben-Jakob E, Cohen I, Shochet O (1995) Novel type of phase transition in a system of self-driven particles. *Phys Rev Lett* 75(6):1226–1229.
17. Inada Y, Kawachi K (2002) Order and flexibility in the motion of fish schools. *J Theor Biol* 214(3):371–387.
18. Couzin ID, Krause J, James R, Ruxton GD, Franks NR (2002) Collective memory and spatial sorting in animal groups. *J Theor Biol* 218(1):1–11.
19. Couzin ID, Krause J, Franks NR, Levin SA (2005) Effective leadership and decision-making in animal groups on the move. *Nature* 433(7025):513–516.
20. Lukeman R, Li YX, Edelstein-Keshet L (2010) Inferring individual rules from collective behavior. *Proc Natl Acad Sci USA* 107(28):12576–12580.
21. Pérez-Escudero A, de Polavieja GG (2011) Collective animal behavior from Bayesian estimation and probability matching. *PLoS Comput Biol* 7(11):e1002282.
22. Ward AJW, Herbert-Read JE, Sumpter DJT, Krause J (2011) Fast and accurate decisions through collective vigilance in fish shoals. *Proc Natl Acad Sci USA* 108(6):2312–2315.
23. Bode NWF, Franks DW, Wood AJ (2011) Limited interactions in flocks: Relating model simulations to empirical data. *J R Soc Interface* 8(55):301–304.
24. Ward AJW, Krause J, Sumpter DJT (2012) Quorum decision-making in foraging fish shoals. *PLoS One* 7(3):e32411.
25. Lopez U, Gautrais J, Couzin ID, Theraulaz G (2012) From behavioural analyses to models of collective motion in fish schools. *Interface Focus* 2(6):693–707.
26. Vicsek T, Zafeiris A (2012) Collective motion. *Phys Rep* 517(3-4):71–140.
27. Weitz S, et al. (2012) Modeling collective animal behavior with a cognitive perspective: A methodological framework. *PLoS One* 7(6):e38588.
28. Pritchard VL, Lawrence J, Butlin RK, Krause J (2001) Shoal choice in zebrafish, *Danio rerio*: The influence of shoal size and activity. *Anim Behav* 62(6):1085–1088.
29. Engeszer RE, Ryan MJ, Parichy DM (2004) Learned social preference in zebrafish. *Curr Biol* 14:881–884.
30. Engeszer RE, Patterson LB, Rao AA, Parichy DM (2007) Zebrafish in the wild: A review of natural history and new notes from the field. *Zebrafish* 4(1):21–40.
31. Buske C, Gerlai R (2012) Maturation of shoaling behavior is accompanied by changes in the dopaminergic and serotoninergic systems in zebrafish. *Dev Psychol* 54(1): 28–35.
32. Hinz FI, Aizenberg M, Tushev G, Schuman EM (2013) Protein synthesis-dependent associative long-term memory in larval zebrafish. *J Neurosci* 33(39):15382–15387.
33. Dreosti E, Lopes G, Kampff AR, Wilson SW (2015) Development of social behavior in young zebrafish. *Front Neural Circuits* 9:39.
34. Pérez-Escudero A, Vicente-Page J, Hinz RC, Arganda S, de Polavieja GG (2014) idTracker: Tracking individuals in a group by automatic identification of unmarked animals. *Nat Methods* 11(7):743–748.
35. Krause J, Tegeder RW (1994) The mechanism of aggregation behaviour in fish shoals: Individuals minimize approach time to neighbours. *Anim Behav* 48(2):353–359.
36. Viscido SV, Miller M, Wethey DS (2002) The dilemma of the selfish herd: The search for a realistic movement rule. *J Theor Biol* 217(2):183–194.
37. Viscido S, Parrish JK, Grünbaum D (2004) Individual behavior and emergent properties of fish schools: A comparison of observation and theory. *Mar Ecol Prog Ser* 273:239–249.
38. Viscido SV, Parrish JK, Grünbaum D (2005) The effect of population size and number of influential neighbors on the emergent properties of fish schools. *Ecol Modell* 183(2-3):347–363.
39. Reluga TC, Viscido S (2005) Simulated evolution of selfish herd behavior. *J Theor Biol* 234(2):213–225.
40. Kimbell HS, Morrell LJ (2015) 'Selfish herds' of guppies follow complex movement rules, but not when information is limited. *Proc Biol Sci* 282(1816):20151558.
41. Orger MB, Kampff AR, Severi KE, Bollmann JH, Engert F (2008) Control of visually guided behavior by distinct populations of spinal projection neurons. *Nat Neurosci* 11(3):327–333.
42. Ahrens MB, et al. (2012) Brain-wide neuronal dynamics during motor adaptation in zebrafish. *Nature* 485(7399):471–477.
43. Severi KE, et al. (2014) Neural control and modulation of swimming speed in the larval zebrafish. *Neuron* 83(3):692–707.